Snow-to-Liquid Ratios Associated with a Strong November Snowstorm:
A Microphysical Analysis

ZACHARY P. UTTECH
NOAA/National Weather Service Great Falls, Montana

ABSTRACT

Five microphysical variables were examined to find their correlation with snow-to-liquid ratios (SLRs) measured at the National Weather Service (NWS) Great Falls, Montana (TFX) office during a strong November snowstorm. The main objectives were to: 1) Find which variables correlated most strongly with SLR, 2) Hypothesize, through a microphysical analysis, as to why the storm averaged 48-hr SLR of 14:1 which was relatively low compared to the NWS TFX forecast of 20:1, and 3) Expose significant variation in SLR throughout this event. Data from four NWS TFX soundings were acquired and examined; 12-hr averaged SLRs were calculated and were centered on sounding release times. After the DGZ (dendritic growth zone) depths were determined, average values for relative humidity (RH_{DGZ}), mixing ratio (g/kg), and precipitable water (inches) were calculated in these layers. This study found several variables with a better correlation with SLR than DGZ depth which had one of the lowest correlations (r=–0.43), and the only one that was negative. Correlation statistics for RH_{DGZ}, of (r=0.24) and (r^2=0.06), were very low. Only 6% of the total variation in SLR was explained by RH_{DGZ}. Linear relationships (with SLR) were much higher for average mixing ratio (r=0.95) and precipitable water (r=0.89). Surface–800 mb RH ($RH_{lowlevel}$) was studied independent of the DGZ for most–but not all–of the storm event. The combination of RH_{DGZ} in the mid to upper 80s (%) and $RH_{lowlevel}$ in the mid to upper 90s (%) favored the highest SLRs.

---

1. Introduction

1.a Background

On November 9th and 10th 2012, a significant snowstorm affected a large portion of Montana. North-central Montana was one of the hardest hit areas in the state. The National Weather Service (NWS) Great Falls WFO officially measured 14.0 inches of snowfall in 24 hours – which ranked 3rd overall, but 1st for the month of November. The average snow-to-liquid ratio (SLR) during this event was 14:1, slightly below the climatological average (1971-2000) of ~17:1 (Baxter et al. 2005) and well below the NWS Great Falls event specific forecast value of 20:1. The SLR showed considerable variation at different stages throughout this storm. Over a 48 hour period, 12-hr average SLRs varied from a high of 16:1 to a low of 6:1.

1.b Literature review and motivation

Previous research has proven that low to mid-level relative humidity influences SLR and is an important variable to consider for snowfall forecasting. A principal component analysis (PCA)[1] performed by Roebber et al. (2002) found SLR to be influenced by seven microphysical factors—

[1] The objective of PCA is to reduce a set of correlated variables to a smaller number of factors, whose linear relationship with the dependent variable is quantified through a regression analysis. The extracted factors are constrained to be orthogonal so there is zero correlation amongst the independent variables (Roebber and Bruening 2002). For this case, the independent variables are a variety of microphysical factors, the dependent variable is the SLR.

one of these factors was low- to mid-level relative humidity (RH). In his paper, the low to mid-level RH was defined to be roughly in the surface–750 mb layer, and the mid-level RH layer was approximately in the 750–600 mb layer. In snowfall events, the low-level tropospheric layer would not include the middle to upper portion of the dendritic growth zone (DGZ), and the mid-level layer would miss the lower portion of the DGZ. Therefore, Roebber's research did not focus on the importance of RH solely within the DGZ and its effect on SLR.

Additional studies have solidified the significance of RH in the DGZ on crystal structure type development and resultant SLR of fallen snow. For example, previous research found that in-cloud temperature and the degree of supersaturation determine ice crystal habit or type (Magono and Lee 1966; Hobbs 1975; Stoelinga et al. 2007; Bailey and Hallett 2009). Furthermore, Roebber et al. (2003) stated that snowfall accumulation is highly dependent on the snow density, which is partially determined by the ice crystal habit and riming accumulated during descent. There are a variety of other factors that govern SLR some of which include: ice crystal growth rates and their size (Takahashi et al. 1991; Ryan 1976 et al.), and sub-cloud processes such as sublimation, melting, and compaction on the ground (Roebber et al. 2003). Past studies by Byers (1965) and Liebbrecht et al. (1999) have determined that ice crystal growth is maximized with in-cloud temperatures near –15°C. Dendritic crystals formation occurs in the –12°C to –18°C isothermic layer; these crystal types are often associated with high SLRs of 20:1 or greater due to air pockets which form between individual crystals as they accumulate on the ground, (see Appendix A and B).

Forecasting SLR is inherently difficult. Extreme SLR values can range from 3:1 to 100:1 (Power et al. 1964; Super and Holroyd 1997; Judson and Doesken 2000; Roebber et al. 2003). Climatological SLRs range across the U.S. with values near 17:1 for the Northern Rockies to 9:1 along the East Coast (Baxter et al. 2005). Not only is SLR seasonally and spatial dependent, significant variation, as will be presented in this paper, is often observed at one location throughout the duration of a winter storm event. The research of this case study focuses on the relationship between DGZ microphysics and SLR. While it only examines one case, it may serve as the impetus for additional study using a larger sample size.

2. Data and Methodology

2.a Data sources

NWS Great Falls (TFX) sounding data was analyzed to determine what factors, despite cold surface temperatures throughout the storm and a cold low- to mid-level tropospheric column during the final two stages of the storm (Fig. 1.c and 1.d), resulted in relatively low SLRs compared to the NWS forecast SLR of 20:1. The sounding data were gathered from the University of Wyoming website (http://weather.uwyo.edu/upperair/sounding.html). SLRs were calculated, using WFO Great Falls snowfall measurements and corresponding liquid precipitation accumulation from the Great Falls Airport ASOS (Automated Surface Observing System), both at 6-hr intervals over a 48-hr period beginning on 11/8/2012 at 18Z and ending on 11/10/2012 at 18Z. Four 12-hr SLRs (12-hr SLR referred to as SLR from here on) were then derived through the averaging of two 6-hr SLRs – one that encompassed the 6 hours preceding a TFX sounding time and the other from the subsequent 6-hr interval (refer to Table 1).

TFX Sounding Release Times	12-hr SLR	12-hr Snowfall (inches)	12-hr Liquid Precipitation (inches)	TFX Surface Temperatures (F)
11/9/2012 (00Z)	13:1	9.6	0.75	28
11/9/2012 (12Z)	16:1	4.4	0.27	22
11/10/2012 (00Z)	9:1	0.7	0.08	13
11/10/2012 (12Z)	6:1	0.7	0.11	6

Table 1. 12-hr Snow-to-liquid ratios centered on TFX sounding release times; accompanying 12-hr snowfall from the NWS Great Falls WFO and liquid precipitation accumulation from the Great Falls Airport ASOS (all units are inches).

2.b Methodology

A variety of microphysical data were examined to determine their influence on SLR including: dendritic snow growth zone depth, relative humidity, mixing ratio, and precipitable water. The data were extracted from within the DGZ layer which is bounded by the –12°C and –18°C isotherms. In this study, the depth of this layer, as defined with respect to pressure, is simply the difference between the corresponding pressure values at the –12°C and –18°C sounding points. In addition to the analysis in the DGZ, average low-level relative humidity in the surface–800 mb layer was examined.

Strongly influenced by the depth of the DGZ as it evolved throughout the storm, were the number of available sounding data points. For the soundings exhibiting the greatest DGZ depth, up to 20 data points were available. On the other end of the spectrum, there were only 3 sounding data points available for analysis when the DGZ vertical depth was most shallow. Python was used for statistical calculations and to create figures 3–7 (each figure shows the evolution of SLR and one of the five analyzed variables).

3. Results

3.a Lower- to middle-tropospheric temperature and moisture progression

Figure 1 contains four TFX sounding profiles. The DGZ on these sounding profiles is represented by the portion inside the solid red lines. The majority of the snowfall during this event, 14.0 inches out of 15.4 inches, occurred between 08/18Z and 09/18Z; thus, most of the snow fell in a tropospheric thermal structure similar to the soundings plotted in 1.a and 1.b. During the heart of the storm, the sounding profiles show a relatively high degree of saturation from near the surface up to approximately 650 mb — a region where temperatures were between –10°C and –5°C, which are conducive for column and needle snow crystal development (Liebbcht et al. 1999). Typically, column and needle crystals are supportive of lower snow-to-liquid ratios compared to dendritic crystals. Analysis of plots 1.a and 1.b also exposed a relatively small DGZ depth of around 50 mb, but yet the highest 12-hr average SLRs of 13:1 and 16:1 were observed during this time.

Temperature advection and diabatic effects (e.g. evaporative cooling) can drastically alter the depth of the DGZ. As the storm progressed, the lower tropospheric temperature profile cooled substantially causing a notable shift of the vertical thermal profile when comparing plots 1.b, 1.c, and 1.d. Persistent cold air advection in the surface to 650 mb layer, as is demonstrated through the comparison of plots 1.b and 1.c, had significant implications on the depth of the DGZ (50 mb → 244 mb) and on the potential for significant changes in SLR observed at the surface. Note how, by this time, the DGZ extends from the surface up to 600 mb (1.c). Cold air advection continued to cool lower tropospheric temperatures during the final stages of the storm (1.c and 1.d), causing the sounding profile to shift to the left of the DGZ. During this transition, the DGZ depth dropped from 244 mb → 78 mb. Examination of the degree of saturation in each sounding plot revealed a layer of lower RH in the sub-cloud region on plot 1.a (compared to 1.b), and a prominent decrease in mid- and upper-level relative humidity (surface–650 mb) in plots 1.c and 1.d. The average relative humidity in the DGZ decreased as well. Detailed microphysical results within the DGZ will be presented in the subsequent section.

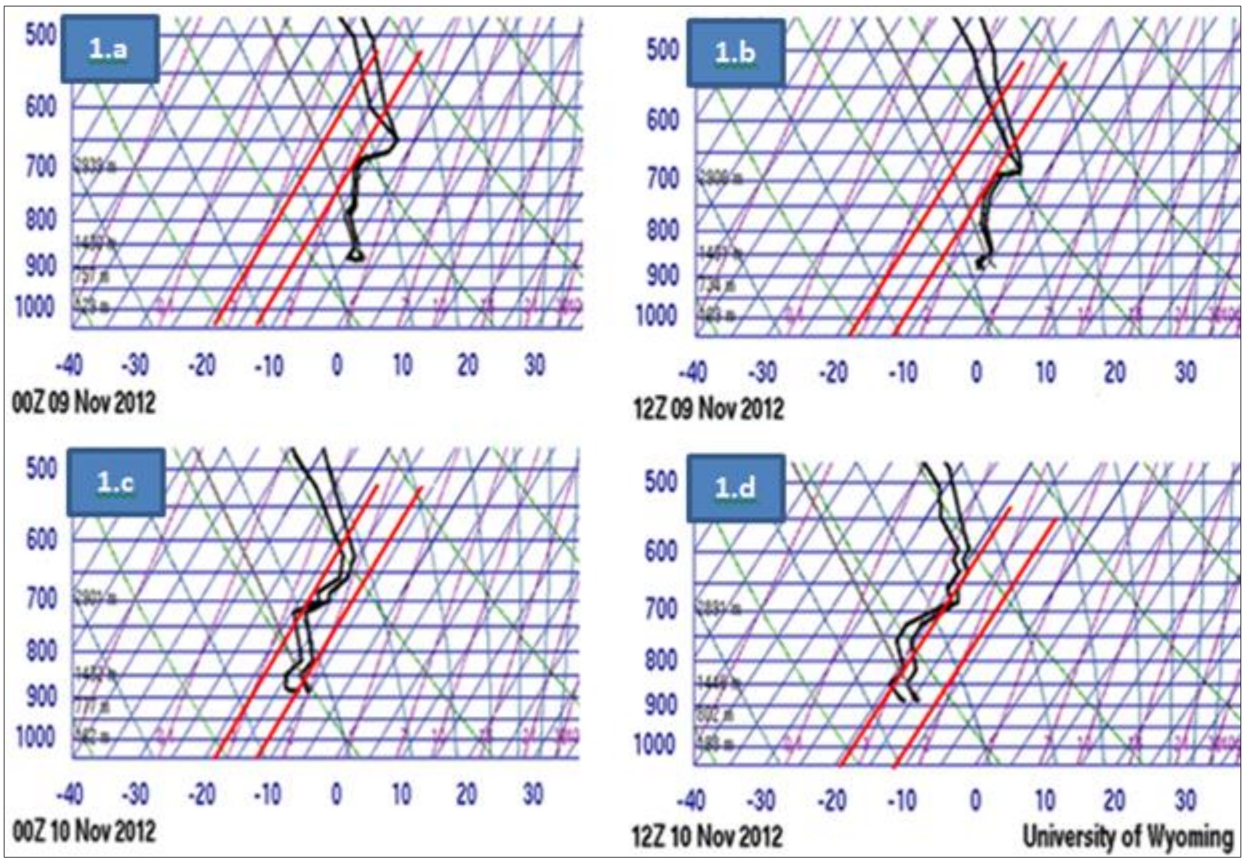

Figure 1. Four TFX sounding plots, (1.a) – (1.d), illustrating the progression of the low- to mid-level temperature and relative humidity, and dendritic snow growth (DGZ) depth. The DGZ is indicated by the area between the two solid red lines. The left most line represents the –18°C isotherm, while the right most line is the –12°C isotherm. The DGZ depth began around 50 mb in 1.a and 1.b then increased substantially to near 250 mb in 1.c, and finally decreased to approximately 80 mb in 1.d.

3.b Microphysical progression in the dendritic growth zone

Out of the four variables studied within the DGZ and plotted in Figure 2, the mixing ratio and precipitable water displayed the best positive correlation with SLR. For an easier description of the progression of the microphysical variables, the storm was separated into four storm phases. The result was one phase for each 12-hr period, all of which are centered on a TFX sounding release time. The four phases resulted in three phase transitions (1→2, 2→3, 3→4). RH_{DGZ} (average relative humidity in the DGZ) was the only variable that increased from phase 1 to phase 2, following the trend of SLR. Mixing ratio and precipitable water decreased for all phase transitions, matching up with the SLR trend for the 2nd and 3rd transitions, but not for the 1st transition, when SLR increased. Precipitable water and mixing ratio were highest during phases 1 and 2, with substantive drops noted during phases 3 and 4. Somewhat surprisingly, the DGZ depth showed poor correlation with SLR, by decreasing slightly through the 1st phase transition. Then, while SLR decreased, the DGZ depth increased considerably through the 2nd transition. Sign changes of DGZ depth and SLR did match up for the final phase transition (3–4), however. The depth of the DGZ was actually the largest (244 mb and 78 mb) during phases 3 and 4 when the SLRs were the lowest at 9:1 and 6:1.

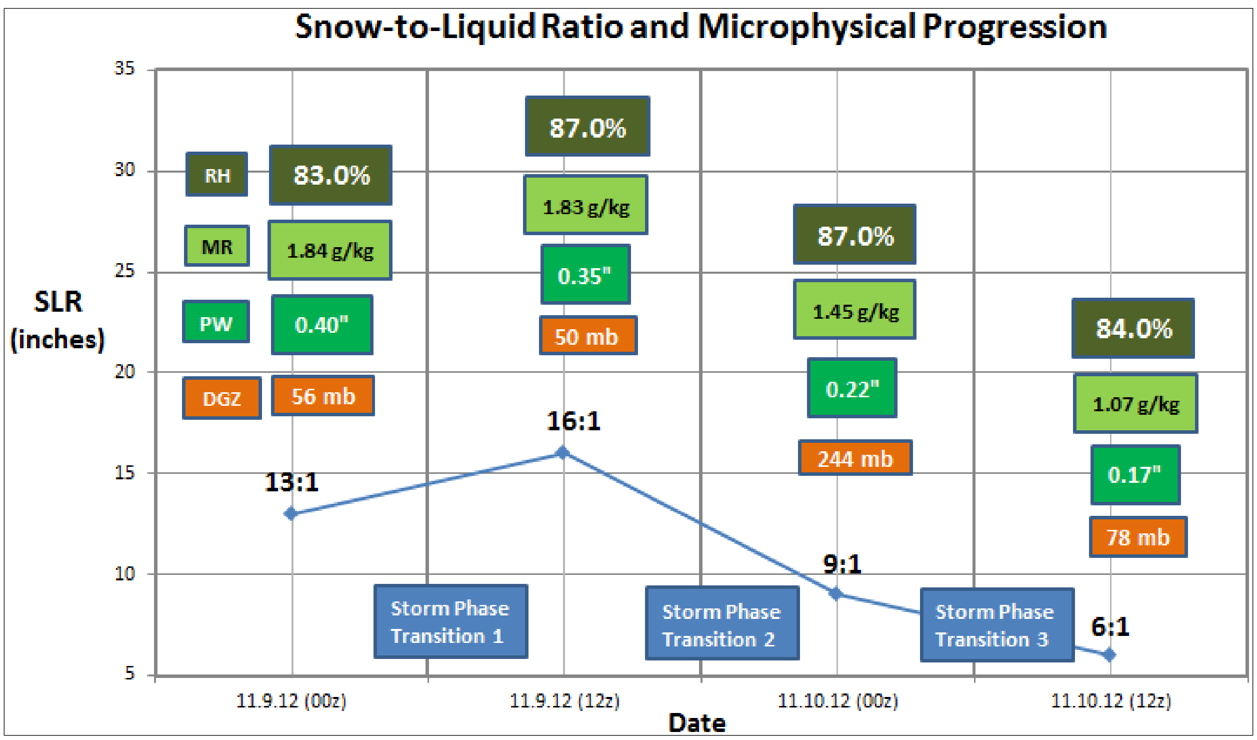

Figure 2. 12-hr average snow-to-liquid ratio progression through the storm duration. Also, plotted are corresponding relative humidity (RH_{DGZ}), mixing ratio (MR), precipitable water (PW), and dendritic snow growth zone (DGZ) depth. RH, MR, and PW are average values from within the DGZ.

The average RH_{DGZ} through all four storm phases, encompassing 48-hrs, was only 85%. Further analysis of Figure 2 reveals subtle changes in RH_{DGZ} throughout the storm, the greatest of which was a 4% increase (83.0% to 87.0%) during the 1st phase transition. The most significant change in RH_{DGZ} did happen to line up with the only increase in SLR (1st phase transition). However, since RH_{DGZ} did not seem to have much bearing on SLR from this point forward, average RH in the surface–800 mb layer ($RH_{lowlevel}$) was examined in an attempt to find a better correlation with SLR; which in fact was found to have a high correlation with SLR. The highest SLRs of 13:1 and 16:1 coincided with $RH_{lowlevel}$ of 94% and 96%, respectfully. Furthermore, the $RH_{lowlevel}$ values during phases 3 and 4 (both at 84%) corresponded with the lowest SLRs of 9:1 and 6:1. Correlation statistics between the five microphysical variables and SLR will be presented in the next section.

Little time was spent analyzing the effect of wind on SLRs as lower tropospheric winds were relatively light through the duration of the storm. Wind speeds from the surface up through the lower troposphere (surface–700mb), were relatively light and more than likely did not create significant fracturing of dendritic aggregates during any of the storm phases (refer to Appendix C for more details).

3.c Correlation statistics

The evolution of SLR and each individual microphysical variable studied are plotted separately in figures 3–7. A cursory look at the four plots concludes that there is a positive correlation between the precipitable water, mixing ratio, and RH_{DGZ}. The correlation coefficient (r) and coefficient of determination (r^2) of these variables with SLR are included in Table 2. The mixing ratio and precipitable water had relatively high (r) values of 0.95 and 0.89. A surprisingly low (r) of 0.24 was found with the RH_{DGZ}. The erratic behavior of the DGZ depth resulted in a negative (r) of –0.43.

As previously mentioned, the $RH_{lowlevel}$ may have played a crucial role in SLR determination and was the one variable studied independent of the DGZ. The higher SLRs of 13:1 and 16:1 coincided with very high RH values of 94% and 96%. On the other hand, lower SLRs of 9:1 and 6:1 corresponded with much lower RH both of 84%. The (r) value for $RH_{lowlevel}$ and SLR is 0.95 (and r^2 is 0.90) which ties with the mixing ratio for the highest (r) and (r^2) values in this study.

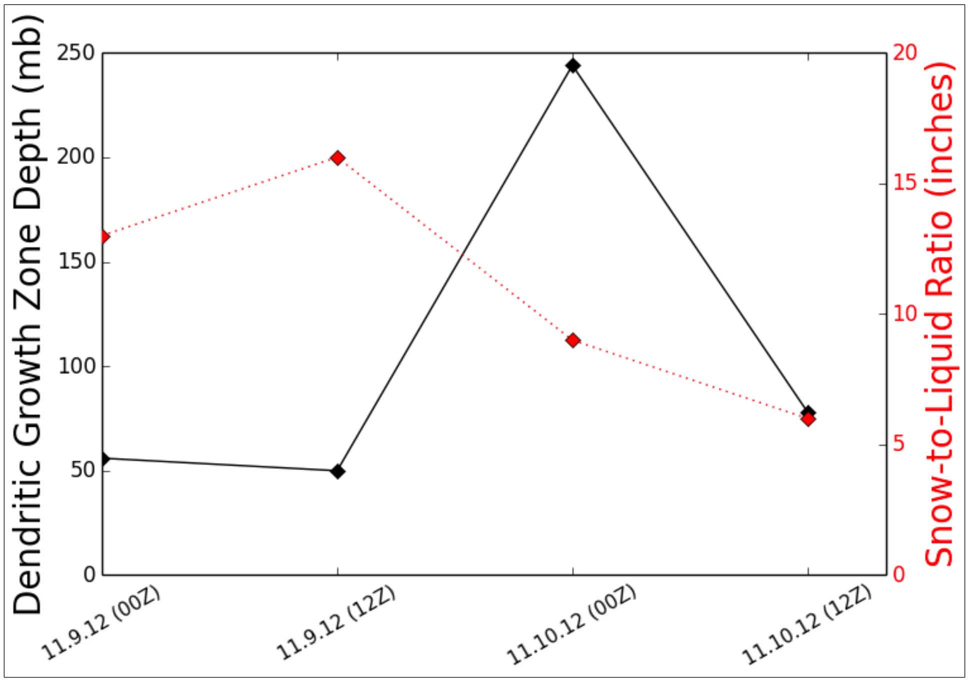

Figure 3. Time evolution of the dendritic growth zone depth (DGZ; mb) and the 12-hr average snow-to-liquid ratio (SLR; inches). In this graph, the DGZ appears to be poorly correlated with the SLR. With the exception of the SLR, all data - were taken from TFX soundings profiles and are average values within the DGZ.

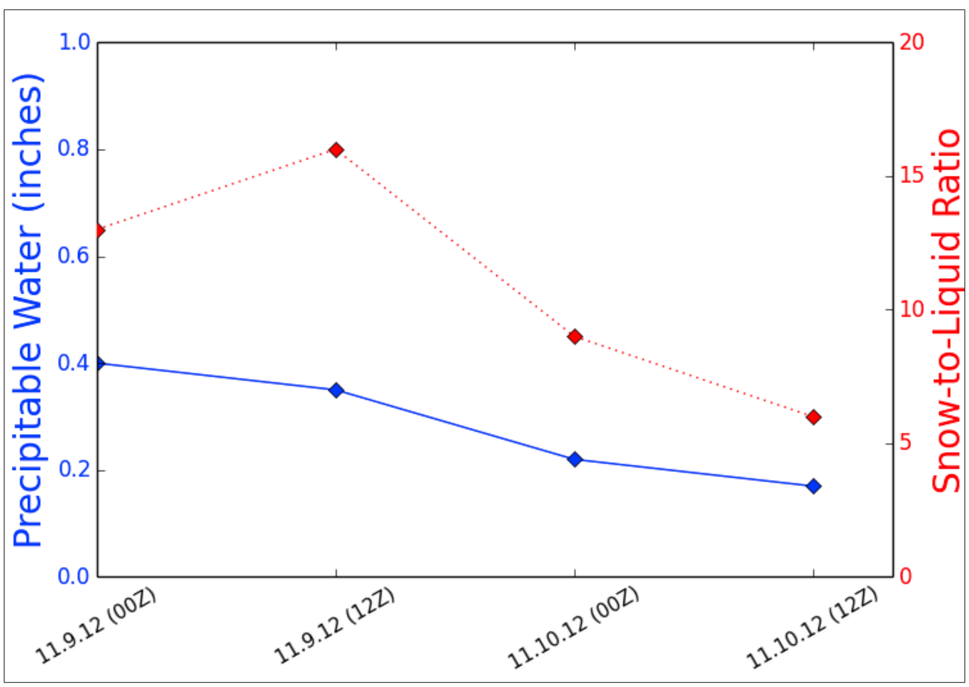

Figure 4. As in Figure 3, but with precipitable water (inches). In this graph, the precipitable water exhibits positive correlation with SLR through their decrease in

value with increasing time.

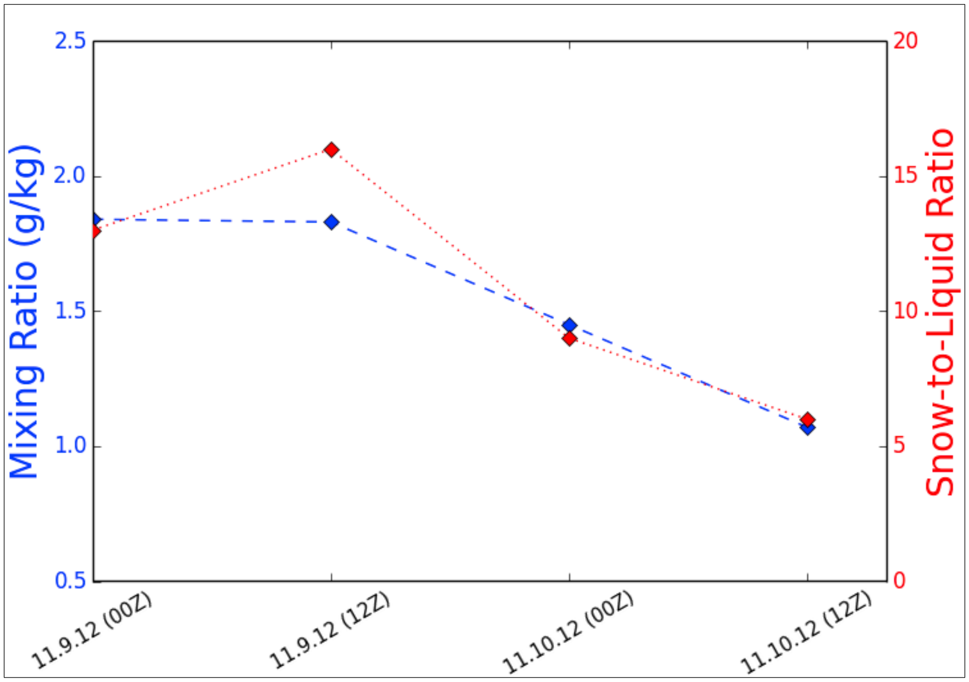

Figure 5. As in Figure 3, but with mixing ratio (g/kg). In this graph, the mixing ratio shows positive correlation with SLR.

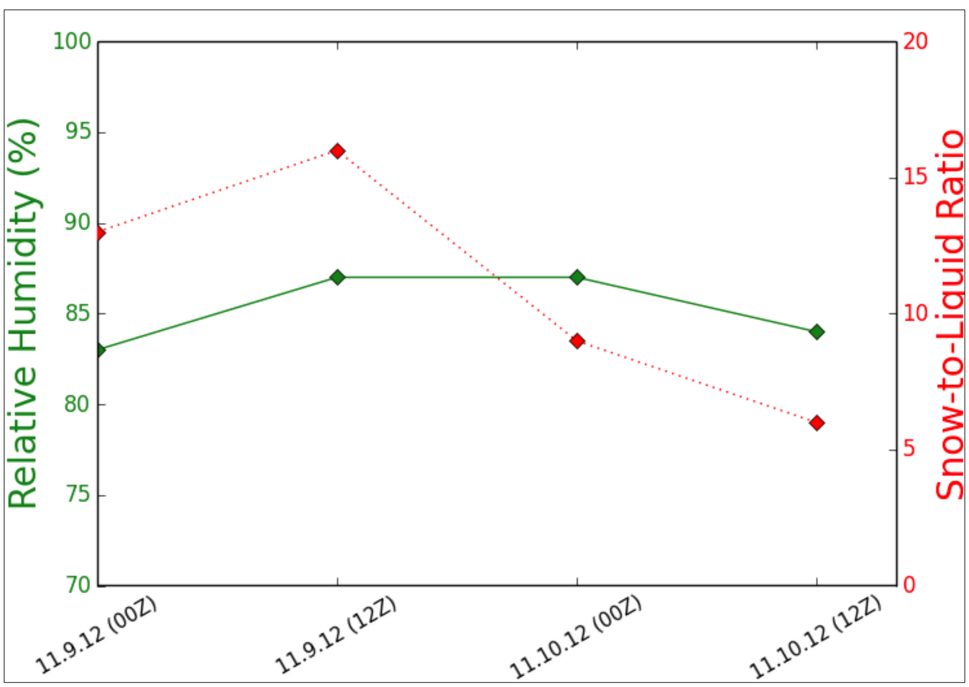

Figure 6. As in Figure 3, but with DGZ relative humidity (%). In this graph, the relative humidity shows lower positive correlation (than precipitable water or

mixing ratio) with SLR.

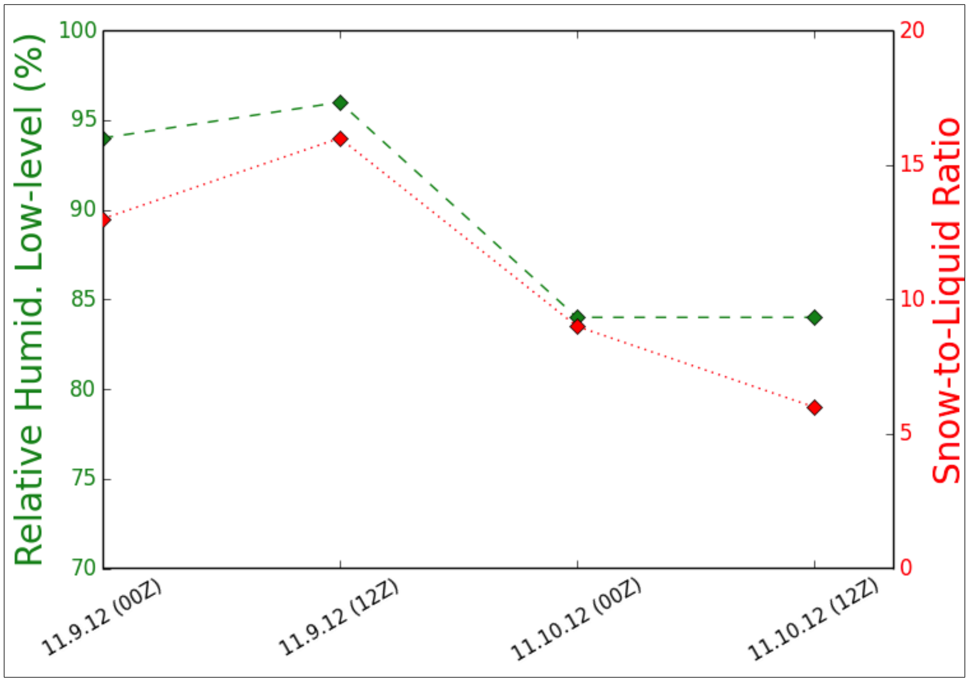

Figure 7. As in Figure 3, but with low-level relative humidity (%). In this graph, the low-level relative humidity displays high positive correlation with SLR (similar to MR).

Variable	r	r^2
RH_{DGZ}	0.24	0.06
$RH_{lowlevel}$	**0.95**	**0.90**
MR	**0.95**	**0.90**
PW	**0.89**	**0.79**
DGZ	-0.43	0.18

Table 2. Correlation coefficient (r) and coefficient of determination (r^2) for five microphysical variables over a 48-hr period.

4. Discussion and summary

NWS forecasters often use DGZ depth as a proxy for SLR; however, in line with previous research, this study exposed the importance of several other atmospheric variables for predicting SLR. Surprisingly among the five variables studied, DGZ depth had one of the lowest correlations (r = –0.43), and the only one that was negative. Prior to this study, the author assumed that in addition to DGZ depth, the average RH within the DGZ would show a strong positive correlation with SLR (increasing RH or supersaturation favor dendrite formation, Liebbrecht et al. 1999). Correlation statistics, at least for this case study, proved this assumption to be false, as (r) was very low at 0.24 (r^2=0.06). Interpretation of the low r^2 value illustrates that 6% of the total variation in SLR can be explained by a linear relationship with RH_{DGZ} with 94% of the total variation in SLR remaining unexplained. However, correlation statistics were much higher for average mixing ratio and precipitable water in the DGZ at (r)=0.95 (r^2=0.90) and (r)=0.89 (r^2=0.79). These two variables had a strong positive correlation with SLR, and 90% of the total variation in SLR can be explained by a linear relationship with mixing ratio and 79% with precipitable water.

This study raised several intriguing questions: why did the highest SLRs of 13:1 and 16:1, during the first two storm phases, match up with the lowest DGZ depths and what factors kept 12-hr average SLRs below the NWS forecast of 20:1? Analysis of the moisture or relative humidity progression, along with a detailed analysis of the average surface-800 mb RH, provided insight into the atypical DGZ depth and SLR correlation. This storm was characterized by a relative mild lower tropospheric temperature profile during the height of the event when the majority of the 15.4 inches fell. A temperature profile warmer than -12C was found in the surface–650mb layer on the 9/10 at 00Z and 9/10 12Z soundings. This meant the majority of the sounding was too warm to be within the DGZ, a result that kept SLR lower than they otherwise would have been. Deep tropospheric cold air advection caused the vertical temperature profile to cool enough for a much larger portion to fall within the DGZ. However, the increased DGZ depth was offset by the lower RH, especially the low-level RH, in the surface-800mb layer. Sub-cloud or near ground level sublimation may be paramount to snow crystal morphology before reaching the ground. Furthermore, higher RH in the lower cloud layer or sub-cloud layer will likely increase precipitation efficiency through mitigation of sublimation effects. This may have resulted in falling SLRs to 9:1 and 6:1 during the final storm phases (1.c and 1.d).

A few points to take away from this analysis, there are many more factors than just the DGZ depth that influence SLR. Significant changes in SLR and DGZ depth are possible through a storm event, so a universal SLR forecast for a storm event may be an over generalization. Although DGZ depth is one of the most popular variables used from SLR forecasting, this study found several with a better correlation with SLR. These variables may be used as a proxy for predicting changes in SLR throughout a storm. More specifically, the combination of RH_{DGZ} in the mid to upper 80s (%) and $RH_{lowlevel}$ in the mid to upper 90s (%) was a set up that favored higher SLRs. As was presented during the second and third storm phase transitions, when one or both of these variables dropped so did the SLR. Future work would entail the acquisition of additional cases studies and comparison of microphysical variable correlation with SLR to the results from this study. Additionally, more data could potentially provide significance to the correlation statistics presented. **A caveat to note: this study did not assess whether a negative omega max and DGZ intersection influenced SLR as it is beyond the scope of this paper; but may be worthy of future work.**

References

Bailey, M. P., and J Hallett, 2009: A comprehensive habit diagram for atmospheric ice crystals: Confirmation from the laboratory, AIRS II, and other field studies. *J. Atmos. Sci.*, **66,** 2888-2899.

Baxter, M. A., C. E. Graves and J. T. Moore, 2005: A climatology of snow to liquid ratio for the contiguous United States. *Wea. Forecasting*, **20,** 729-744.

Byers, H. R., 1965: Elements of Cloud Physics. *University of Chicago Press*, 191 pp.

Hobbs, P. V., 1975: The nature of winter clouds and precipitation in the Cascade Mountains and their modification by artificial seeding. Part I: Natural conditions. *J. Appl. Meteor.*, **14,** 783-804.

Judson, A., and N. Doesken, 2000: Density of freshly fallen snow in the central Rocky Mountains. *Bull. Amer. Meteor. Soc.*, **81,** 1577–1587.

Liebbrecht, K. G., and V. M. Tanusheva, Phys. Rev. Lett. **83**, 1699 (1999).

Magono, C., and C. Lee, 1966: Meteorological classification of natural snow crystals. *J. Fac. Sci. Hokkaido Univ. Ser. 7*, **2,** 321-335.

Power, B. A., P. W. Summers, and J. d' Avignon, 1964: Snow crystal forms and riming effects as related to snowfall density and general storm conditions. *J. Atmos. Sci.*, **21,** 300-305.

Roebber, P. J., and S. L. Bruening, 2002: Improving snowfall forecasting by diagnosing snow density. *Wea. Forecasting*, **18,** 264-287.

——, S. L. Bruening, D. M. Schultz, and J. V. Cortinas, 2003: Improving snowfall forecasting by diagnosing snow density. *Wea. Forecasting*, **18,** 264-287.

Ryan, B. F. D., E. R. Wishart, and D. E. Shaw, 1976: The growth rates and densities of ice crystals between -3°C and -21°C. *J. Atmos. Sci.*, **33,** 842-850.

Stoelinga, J. D. Locatelli, and C. P. Woods, 2007: The occurrence of "irregular" ice particles in stratiform clouds. *J. Atmos. Sci.*, **64,** 2740-2750.

Super, A. B., and E. W. Holroyd III, 1997: Snow accumulation algorithm for the WSR-88D radar: Second annual report. U.S. Department of Interior Bureau Reclamation Tech. Rep. R-97-05, U.S. Dept. of Interior, Denver, CO, 77 pp.

Takahashi, T., T. Endoh, and G. Wakahoma, 1991: Vapor diffusional growth of free-falling snow crystals. *J. Meteor. Soc. Japan*, **69,** 15-30.

University of Wyoming, Atmospheric Sci., (http://weather.uwyo.edu/upperair/sounding.html).

Appendix A (Normalized ice crystal growth rate as a function of temperature, Byers 1965).

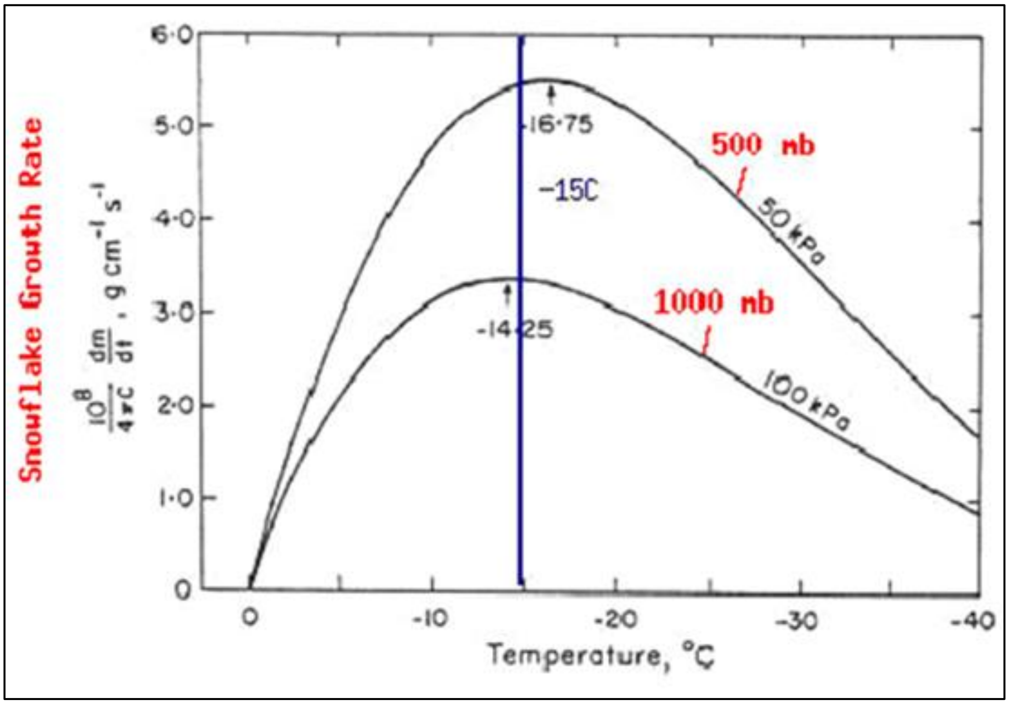

Appendix B (Liebbrecht et al. 1999)

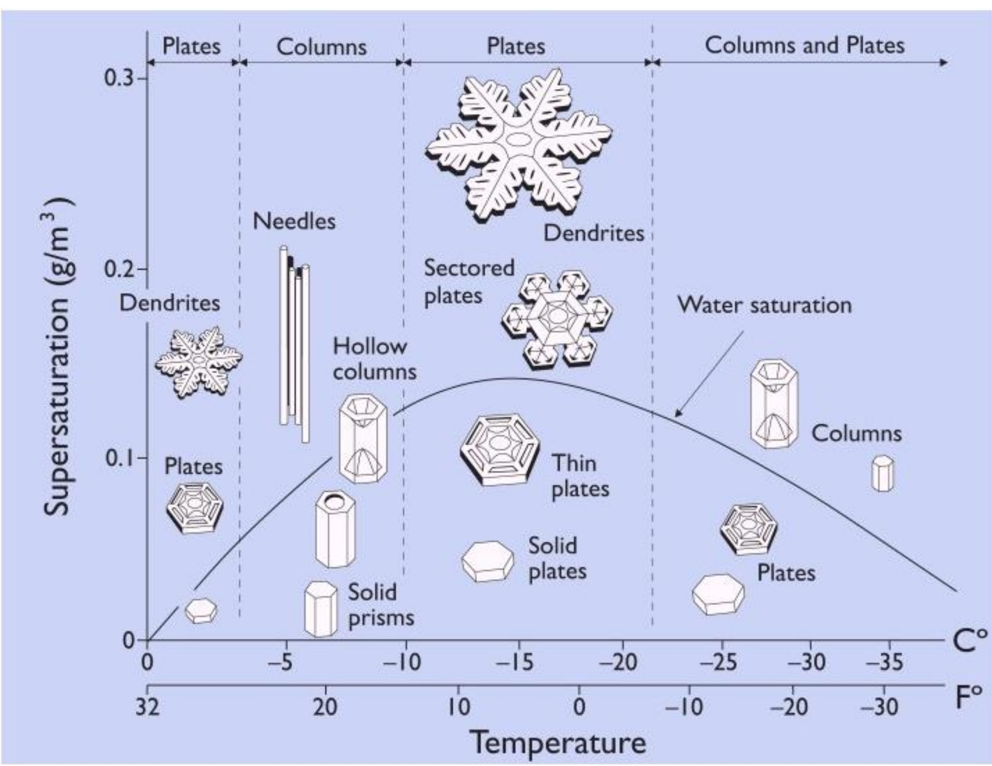

Appendix C. Correlation coefficient (r) and coefficient of determination (r^2) for surface to 700mb average wind speed with SLR. Wind and SLR data was acquired from four TFX soundings (Table C.2).

Variable	**r**	**r^2**
Sfc-700mb Average Wind Speed	−0.07	0.004

Table C.1

TFX Sounding	11/9/2012 (00Z)	11/9/2012 (12Z)	11/10/2012 (00Z)	11/10/2012 (12Z)
SLR	13:1	16:1	9:1	6:1
Wind $Speed_{avg\ sfc\text{-}700mb}$ (kts)	16	6	13	8

Table C.2